

# Collapse-reexpansion conformational transition of alginate under non-specific ion conditions

Xiaoyang Li<sup>1</sup>, Yi Wang<sup>1</sup>, Cuixia Sun, Yiguo Zhao, Wei Lu, Yapeng Fang<sup>\*</sup>

School of Agriculture and Biology, Shanghai Jiao Tong University, 800 Dongchuan Road, Shanghai, 200240, China

## ARTICLE INFO

### Keywords:

Alginate  
Molecular conformation  
Non-specific metal ion  
Electrostatic screening effect  
Overcharging

## ABSTRACT

As negatively charged polyelectrolytes, alginate conformation is greatly influenced by ionic environment, which is of critical importance for solution properties and practical applications. To advance our understanding of alginate conformation in the presence of non-specific ions (NaCl, KCl, MgCl<sub>2</sub>), high resolution atomic force microscopy, together with statistical analysis, is employed to provide direct structural information. Alginate chains undergo a collapse-reexpansion transition with increasing salt concentration, which is quantitatively evidenced by a nonmonotonic evolution of persistence length ( $L_p$ ). At low salt concentrations, a decrease in  $L_p$  is caused dominantly by electrostatic screening effect as electrostatic persistence length ( $L_p^0$ ) shows a strong dependence on Debye screening length ( $\kappa^{-1}$ ) with a scaling relation of  $L_p^0 \sim \kappa^{-2}$ , which is in agreement with Odijk-Skolnick-Fixman theory described for semiflexible polyelectrolytes. Above a certain salt concentration, there is a rise in  $L_p$ , which can be explained by overcharging and ion-ion correlations. The type of salt also affects the change degree of persistence length, with divalent ions (Mg<sup>2+</sup>) showing the greatest collapse and reexpansion level. Since alginate chains containing higher  $\alpha$ -L-guluronate (G) content are more influenced by salts, it can be inferred that non-specific ions have a higher affinity for G units.

## 1. Introduction

Alginate, a natural polysaccharide extracted from brown seaweeds or bacteria, has gained considerable attention over the years, particularly in the fields of food industry and biomedical engineering due to its abundant sources as well as the edible, biocompatible, biodegradable characteristics (Bennacef et al., 2021; Fernando et al., 2020; Varaprasad et al., 2020). Structurally, it is a linear biopolymer consisting of  $\beta$ -D-mannuronate (M) and  $\alpha$ -L-guluronate (G) units (Fig. S1), which are arranged in a blockwise pattern including G-blocks, M-blocks and MG-blocks (Ramdhan et al., 2020; Hecht & Srebnik, 2016). Since each of the two units has a carboxyl group, alginate chains act as negatively charged polyelectrolytes in aqueous solution, of which the conformational properties can be tuned by the presence of salts (Smidsrød et al., 1970; Thu et al., 1996). Calcium ion can promote the cross-linking of alginate, forming the famous egg-box model, which is the underlying mechanism of the gelation of alginate (Cao et al., 2020; Sikorski et al., 2007). In addition to calcium ion, other divalent or multivalent ions can also lead to the gelation of alginate, such as Ba<sup>2+</sup>, Cu<sup>2+</sup>, Sr<sup>2+</sup>, Fe<sup>2+</sup>, Zn<sup>2+</sup>,

Mn<sup>2+</sup>, Al<sup>3+</sup>, Fe<sup>3+</sup>, while monovalent ions such as Na<sup>+</sup> and K<sup>+</sup> ion, as well as some divalent ions such as Mg<sup>2+</sup> cannot, which are known as non-specific metal ions (Donati & Christensen, 2023; Hu et al., 2021; Makarova et al., 2023; Morch et al., 2006). Despite extensive research on alginate to date, the effect of non-specific ions on alginate chain conformation, which is of critical importance for solution properties and practical applications, remains ambiguous.

The conformation of alginate chains, which can be reflected by the solution properties at extremely dilute concentrations, has been studied through many experimental approaches such as light scattering, viscosity and conductivity (Smidsrød & Haug, 1968; Dentinia et al., 2005; Santra & Das, 2019; Smidsrød et al., 1973; Smidsrød & Haug., 1971; Vold et al., 2006). Specifically, based on the relationship between the z-average radius of gyration and the molecular weight, or the relationship between the intrinsic viscosity and the molecular weight, the chain flexibility can be estimated. However, the conformation properties deduced from these approaches cannot reach a consensus. For example, the results obtained from light scattering and viscosity gave the conclusion that the relative extension of different alginate blocks

\* Corresponding author.

E-mail addresses: [lixiaoyang@sjtu.edu.cn](mailto:lixiaoyang@sjtu.edu.cn) (X. Li), [wangyi51@sjtu.edu.cn](mailto:wangyi51@sjtu.edu.cn) (Y. Wang), [cxsunphd@sjtu.edu.cn](mailto:cxsunphd@sjtu.edu.cn) (C. Sun), [ygzhaos@sjtu.edu.cn](mailto:ygzhaos@sjtu.edu.cn) (Y. Zhao), [wei.lu@sjtu.edu.cn](mailto:wei.lu@sjtu.edu.cn) (W. Lu), [ypfang@sjtu.edu.cn](mailto:ypfang@sjtu.edu.cn) (Y. Fang).

<sup>1</sup> These authors contributed equally to this work.

<https://doi.org/10.1016/j.foodhyd.2024.110744>

Received 26 August 2024; Received in revised form 25 September 2024; Accepted 12 October 2024

Available online 16 October 2024

0268-005X/© 2024 Elsevier Ltd. All rights reserved, including those for text and data mining, AI training, and similar technologies.

increases in the order “MG-blocks < M-blocks < G-blocks”, while another work proposed that chain extension is independent of their chemical composition (Smidsrød et al., 1973; Smidsrød & Haug., 1971; Vold et al., 2006). Many reasons could account for the discrepancies. For light scattering and conductivity measurements, a limited concentration range is required (Smidsrød & Haug., 1971; Dentinia et al., 2005; Santra & Das, 2019; Vold et al., 2006). However, unless the polymer is in a diluted state, the presence of interchain interactions will interfere with the determination of chain conformation. In some scattering studies, dust particles are difficult to be removed completely, which leads to uncertainty in experimental results (Smidsrød & Haug, 1968; Smidsrød et al., 1973; Strand et al., 1982). Additionally, various theoretical models adopted in different systems might provide different structural information, which could also lead to discrepancies. Thus, it remains essential to accurately capture the molecular conformation of polymer in dilute solutions.

It has been reported that the addition of non-specific metal ions could lead to the collapse of alginate chains (Banerjee et al., 2022). However, such structural transition is derived from viscosity measurements and lacks direct evidence. Here, high resolution atomic force microscopy (AFM) together with statistical analysis is employed to characterize alginate chains, which can not only visualize the chain morphologies directly but also provide detailed chain structural parameters. In our previous work, the pathway of alginate chain growing from single molecule to dimers and further into multimers was successfully followed by AFM imaging upon addition of calcium ions (Wang et al., 2023). Besides, it has also been used to provide direct information on the conformation of other polysaccharides (e.g. iota-carrageenan) and proteins (e.g. amyloid fibrils) (Schefer et al., 2014; Adamcik et al., 2010). The study presented here aims to use AFM imaging to unravel the conformation properties of alginate in dilute solutions as influenced by non-specific ions ( $\text{Na}^+$ ,  $\text{K}^+$ ,  $\text{Mg}^{2+}$ ). Based on the structural transitions of polyelectrolyte chains such as carrageenan and poly (2-vinylpyridine) (Roiter et al., 2010; Schefer et al., 2015), it is hypothesized that alginate chains undergo a collapse-reexpansion transition with increasing salt concentration, accompanied by a nonmonotonic evolution of persistence length. The possible reasons for the conformational transition of alginate chain are addressed.

## 2. Materials and methods

### 2.1. Materials

Two sodium alginates with different guluronate (G) content were purchased from San Ei-Gen FFI Inc. (Osaka, Japan) and Macklin Inc. (Shanghai, China), respectively. In order to eliminate the effect of free salts other than sodium ions, the alginate samples were purified prior to AFM measurements. Specifically, a solution of alginate at a concentration of 10 mg/mL is first prepared, then dialyzed for three days, and finally freeze-dried to obtain purified alginate. The cation contents of the purified alginates were measured by inductively coupled plasma optical emission spectrometer (ICP-OES, iCAP 7600, Thermo Scientific), which showed that the major cation is sodium ion, with  $\text{K}^+$ ,  $\text{Ca}^{2+}$  and  $\text{Mg}^{2+}$  all below 500 ppm (Table S1). The M/G contents of both samples were characterized by  $^1\text{H}$  nuclear magnetic resonance ( $^1\text{H}$  NMR, Avanceo 700 MHz, Bruker), which showed that the G contents are 56% and 25%, and the M contents are 44% and 75%, respectively. Based on the percentage of G content, they were named ALG56 and ALG25, respectively. The weight average molecular weights ( $M_w$ ) of the two alginate samples are similar (225 kDa for ALG56, 226 kDa for ALG25), as determined by gel permeation chromatography coupled with multi-angle laser light scattering (GPC-MALLS, Vis-cotek TDAmx, Malvern) (Wang et al., 2023). Sodium chloride, potassium chloride and magnesium chloride were obtained from Sinopharm Chemical Reagent Co., Ltd. (Shanghai, China) and 3-Aminopropyl triethoxysilane (APTES) was from Beijing InnoChem Science and Technology Co., Ltd (China).

### 2.2. Atomic force microscopy (AFM) measurements

For the sample preparation, dilute alginate solution (1  $\mu\text{g}/\text{mL}$ ) was prepared and subjected to filtration (0.45  $\mu\text{m}$ ), as well as NaCl, KCl,  $\text{MgCl}_2$  aqueous solution (2 M). A certain amount of salt solution was added to alginate solution under constant stirring and the final concentrations of salt were 0, 2, 5, 10, 50, 100 mM. The corresponding mass fraction of alginate and added counterions was shown in Table S2.

The observation of samples was performed on a Multimode 8 Scanning Force Microscope (Bruker, USA). In order to achieve an effective immobilization of alginate chains on the mica surface, APTES was used to convert the charge of mica substrate from negative to positive as the alginate chains are negatively charged. Specifically, APTES solution (0.01% v/v, 20  $\mu\text{L}$ ) was deposited onto a fresh cleaved mica substrate for 30 s, which was then rinsed with 1 mL Milli-Q water for five times and dried by high-purity nitrogen gas. After the modification of mica, the prepared alginate samples (20  $\mu\text{L}$ , 1  $\mu\text{g}/\text{mL}$ ) containing different types and amounts of salts were dripped onto the mica surface for 30 s, which was then washed with 1 mL Milli-Q water, followed by the nitrogen drying.

### 2.3. Zeta potential measurement

The zeta potential of alginate solution with varying salt concentrations was measured by Zetasizer Nano ZS device (Malvern Instruments, U.K.). The alginate concentration was 1  $\mu\text{g}/\text{mL}$ , and the salt concentrations were 0, 2, 5, 10, 50, 100 mM, respectively.

### 2.4. Data analysis

FiberApp, an open-source software, was employed to analyze the average height  $\langle h \rangle$  and persistence length  $L_p$  of alginate chains in AFM images (Usov & Mezzenga, 2015). For statistical analysis, more than 200 alginate chains were traced. The average height was obtained by Gaussian fitting of height histograms, which plots the number of alginate chains versus the mean height of a single alginate chain. The persistence length  $L_p$ , which reflects the flexibility of alginate chains, can be calculated based on the two-dimensional (2D) worm-like chain model:

$$\langle R^2 \rangle = 4L_p(L - 2L_p(1 - \exp(-L/2L_p)))$$

Where  $\langle R^2 \rangle$  is the average square end-to-end distance of alginate chain,  $L$  is the total contour length between two end points.

## 3. Results

### 3.1. The morphology evolution of alginate chains with non-specific metal ions

The morphology of alginate chains with the addition of non-specific metal ions was followed by capturing the AFM images. As shown in Fig. 1, alginate chains in salt-free solution exhibit an expanded structure. As sodium ions were added into the solution, alginate chains showed a conformational transition. At low sodium ion concentrations (from 2 to 10 mM), the chain collapse occurs, forming hairpin and toroid structures. It is worth noticing that there is no multi-chain aggregation even when single chain collapse happens. When sodium ion concentration reaches 50 mM, alginate chains reexpand, but not to the same extent as when no ions are added. The same trend of transition was observed for alginate chains with the addition of KCl and  $\text{MgCl}_2$  (Figs. 2 and 3). For ALG25, which has a low content of guluronate, it was also found that upon addition of non-specific ions, the alginate chain undergoes a collapse transition followed by reexpansion (Fig. S2, S3 and S4).

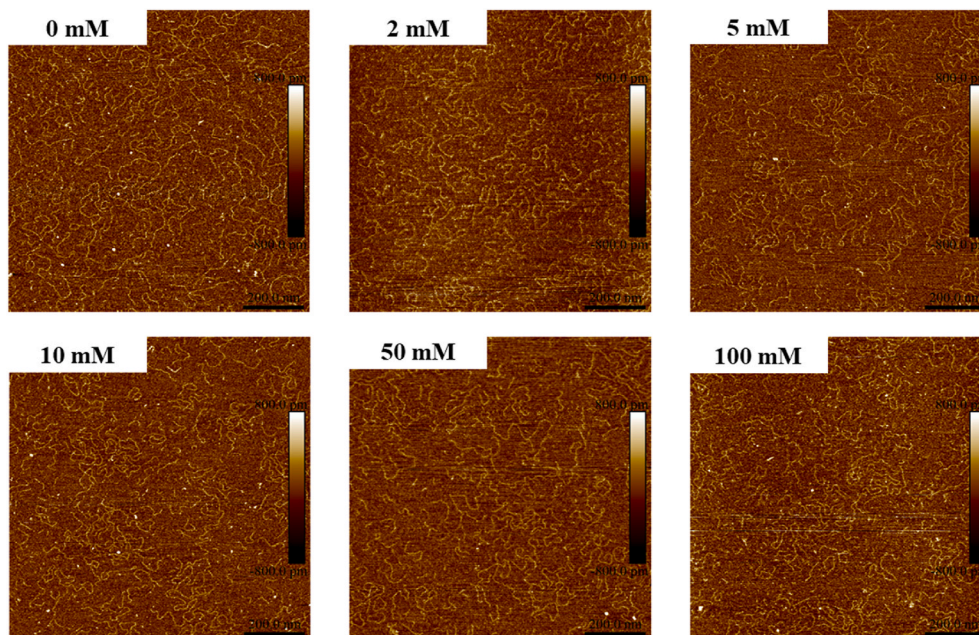


Fig. 1. AFM images of ALG56 at different NaCl concentrations.

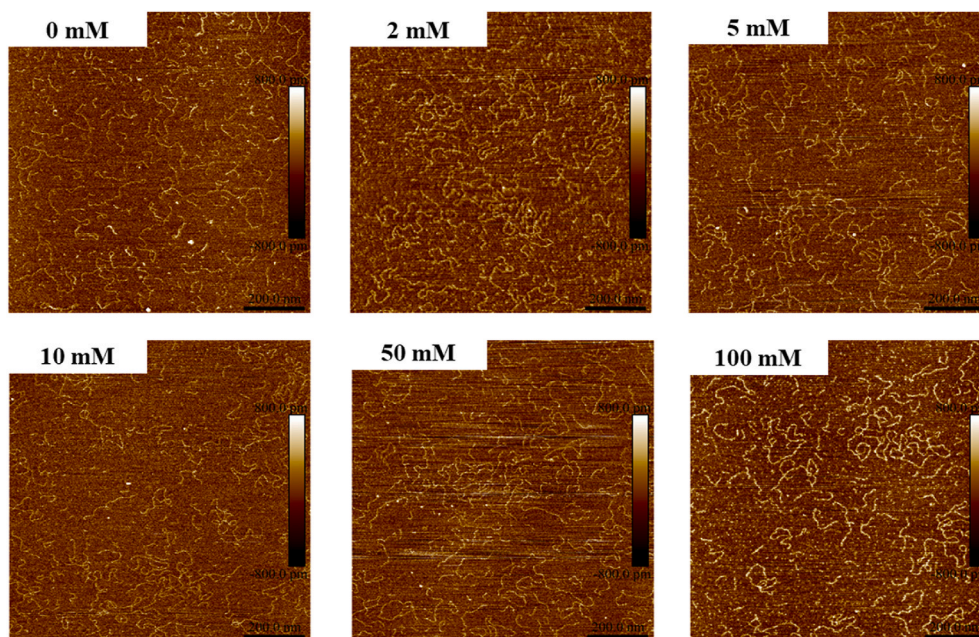


Fig. 2. AFM images of ALG56 at different KCl concentrations.

### 3.2. The effect of non-specific metal ions on the persistence length of alginate chains

The flexibility of alginate chains can be reflected by the persistence length, which is extracted from alginate chain imaged by AFM. As shown in Fig. 4a, the persistence length of ALG56 follows a similar trend with the gradual addition of  $\text{Na}^+$ ,  $\text{K}^+$  and  $\text{Mg}^{2+}$ . It was shown that the persistence length of ALG56 decreases with the addition of salts at concentrations of 0–10 mM, known as the chain-collapse region, while it increases with the salts within a concentration range of 50–100 mM, which is termed as the chain-reexpansion region. Besides, it could be found that at the same salt concentration, the persistence length of alginate chains is greatly affected by the types of salts. When the salt concentration is lower than 10 mM, the persistence length of alginate

chain with  $\text{Na}^+$  ions is higher than that with  $\text{K}^+$  ions, followed by that with  $\text{Mg}^{2+}$  ions; when the salt concentration reaches 50 mM, the persistence length of alginate chain is in the order of  $\text{Mg}^{2+} > \text{K}^+ > \text{Na}^+$ ; in salt-free condition, there is no significant difference in the persistence length of alginate chains with the three types of salts. The variation of the persistence length of ALG25 with the addition of salts follows the same trend as that of ALG56, and the relative magnitude of persistence length is also the same for the addition of the three different types of salt (Fig. 4b).

### 3.3. The effect of non-specific metal ions on the height of alginate chains

Both the type and concentration of salts affect the height of alginate chains. As shown in Fig. 5 and Table S3, at low salt concentrations, the

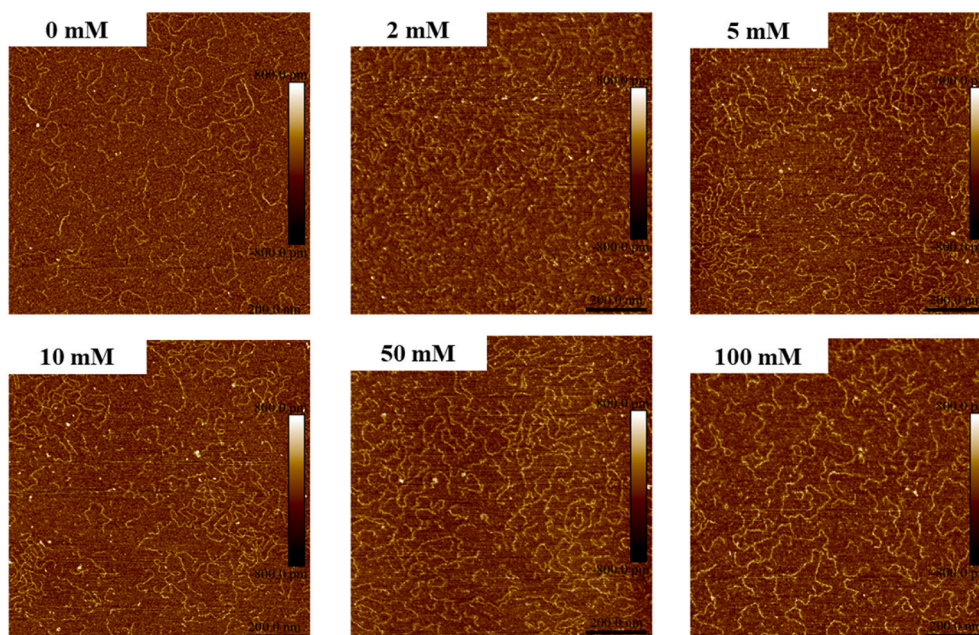


Fig. 3. AFM images of ALG56 at different  $\text{MgCl}_2$  concentrations.

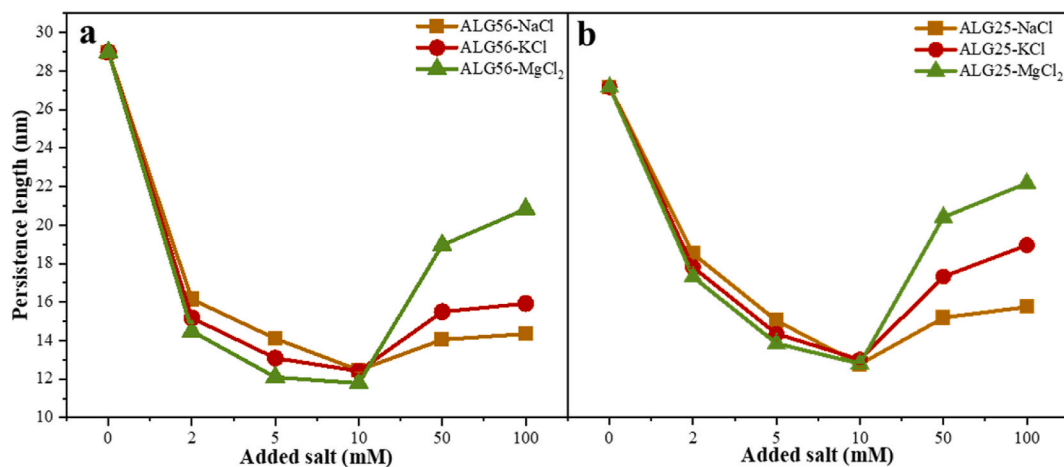


Fig. 4. The persistence lengths of ALG56 (a) and ALG25 (b) as a function of salt concentration.

height of alginate chains has no change, which is close to that in salt-free solution. When the salt concentration increases to a certain value, the height exhibits a slight increase because the volume of the ions cannot be ignored like a point charge. The binding of a large number of ions results in an increase in the volume of the alginate chain. Within the same range of salt concentrations and types studied, there are more samples showing an average height greater than 0.30 nm for ALG56 than for ALG25. At high salt concentrations, the average height of ALG56 is larger than that of ALG25, which suggests that alginate chains with a higher G content have a greater affinity for non-specific ions, leading to a higher height of the alginate chain. Besides, for ALG56, average heights above 0.30 nm appear at lower concentrations of  $\text{Mg}^{2+}$  ions, followed by  $\text{K}^+$  ions, and finally  $\text{Na}^+$  ions, which can be explained by the order of affinity of the ions for alginate, that is,  $\text{Mg}^{2+} > \text{K}^+ > \text{Na}^+$ .

## 4. Discussion

### 4.1. The reduction in persistence length at low salt concentrations

According to the Odijk-Skolnick-Fixman (OSF) theory and Barrat-

Joanny (BJ) theory (Odijk, 1977; Skolnick & Fixman, 1977; Barrat & Joanny, 1993; Barrat & Joanny, 1996), the total persistence length ( $L_p$ ) of polyelectrolytes in a salt solution consists of two parts, that is, the bare persistence length ( $L_p^0$ ) and the electrostatic persistence length ( $L_p^e$ ):

$$L_p = L_p^0 + L_p^e$$

The  $L_p^0$  originates from the local stiffness of the uncharged segment, which is irrespective of the chemical composition of sodium alginate. The  $L_p^e$  is caused by the intrachain electrostatic repulsion, which depends on the ionic strength ( $I$ ) through the Debye screening length ( $\kappa^{-1}$ ). There is a power-law scaling relation between  $L_p^e$  and  $\kappa^{-1}$  (or ionic strength  $I$ ), which is affected by the flexibility of the chain. For semiflexible polyelectrolytes, a relation of  $L_p^e \sim \kappa^{-2} \sim I^{-1}$  has been confirmed by some experimental and simulation studies (Usov et al., 2013; Caliskan et al., 2005), which is consistent with the OSF theory, while for flexible polyelectrolytes, the dependence is weaker (Sim et al., 2012), following a relation of  $L_p^e \sim \kappa^{-1} \sim I^{-1/2}$  according to BJ theory.

To study the scaling relation ( $L_p^e \sim \kappa^{-y}$ ) in alginate system, a dilute condition is required, where interchain interactions can be neglected.

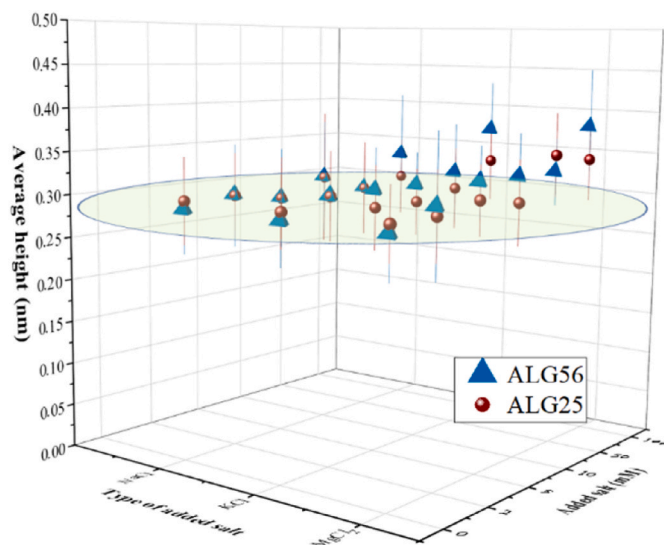


Fig. 5. The average heights of alginate chains under different salt conditions.

Two analytical approaches, volume fraction of alginate chains to total sample and overlap concentration, were employed to demonstrate that alginate chains at a concentration of 1  $\mu\text{g}/\text{mL}$  are in a dilute condition, as described in the Supporting Information (Odijk, 1979; Dobrynin & Rubinstein, 2005; Liao et al., 2003). For the estimation of the scaling relation of alginate chains, the minimum value of the measured persistence length, i.e., 11.70 nm (for ALG56 with 10 mM  $\text{MgCl}_2$ , shown in Table S3), was taken as the  $L_p^0$ . This is close to the previous results obtained by size-exclusion chromatography together with online multi-angle laser light scattering and viscometry, which gave an estimated  $L_p^0$  of 12 nm (Vold et al., 2006). The  $L_p^e$  was then obtained by subtracting  $L_p^0$  (11.70 nm) from the total  $L_p$  (Table S3).

The Debye screening length  $\kappa^{-1}$  can be calculated from ionic strength  $I$  (Cifre & de la Torre, 2014):

$$\kappa^{-1} = 1 / \sqrt{8\pi l_B N_A I}$$

$$I = \frac{1}{2} \sum_i c_i q_i^2$$

where  $l_B$  is Bjerrum length, a solvent property defining a characteristic length scale associated to the strength of the electrostatic interaction, and the Bjerrum length of water at 25  $^\circ\text{C}$  is 0.71 nm (Vold et al., 2006; Odijk, 1979; Manning, 1969),  $N_A$  is the Avogadro number,  $c_i$  is the ion concentration,  $q_i$  is the ion valence. Based on these calculations, linear fitting of the  $\log L_p^e - \log \kappa^{-1}$  plots were carried out, and the y-values were derived from the slopes of the plots, which are all around 2 (Fig. 6). This value is consistent with the OSF theory for semiflexible polyelectrolytes.

The consistency of the scaling relation with OSF theory can also be proved by another method. Since the persistence length (28.98 nm for ALG56, 26.34 nm for ALG25) and the total contour length (150 nm for ALG56, 155 nm for ALG25) of alginate are of the same order of magnitude, alginate chains are expected to behave like semiflexible polyelectrolytes. Assuming a scaling relation of  $L_p^e \sim \kappa^{-2} \sim I^{-1}$  for the semiflexible alginate chain given by the OSF theory, the plot of  $L_p - I^{-1}$  would be linear with an intercept that denotes  $L_p^0$ . As shown in Fig. S5, the  $L_p^0$  values (Avg = 11.59 nm) agree very well with the minimum  $L_p$  (11.70 nm) observed for ALG56 with 10 mM  $\text{MgCl}_2$ .

Therefore, the scaling relation ( $L_p^e \sim \kappa^{-2} \sim I^{-1}$ ) for alginate chains is consistent with the OSF theory, proving a collapsing mechanism dominated by electrostatic screening effect. For alginate in extremely diluted solution, the intrachain electrostatic repulsions hold alginate chains in an expanded state whereas the interchain interactions can be neglected. When salts ( $\text{Na}^+$ ,  $\text{K}^+$  and  $\text{Mg}^{2+}$ ) are added, the Debye screening length gets reduced with the ion strength increasing according to the Debye-Hückel Theory, thus leading to the weakening of the intrachain electrostatic repulsion, and the collapse of alginate chains.

#### 4.2. The increase of persistence length at high salt concentrations

The persistence length of alginate chain increases when the ion concentration reaches 50 mM, which is described as chain reexpansion.

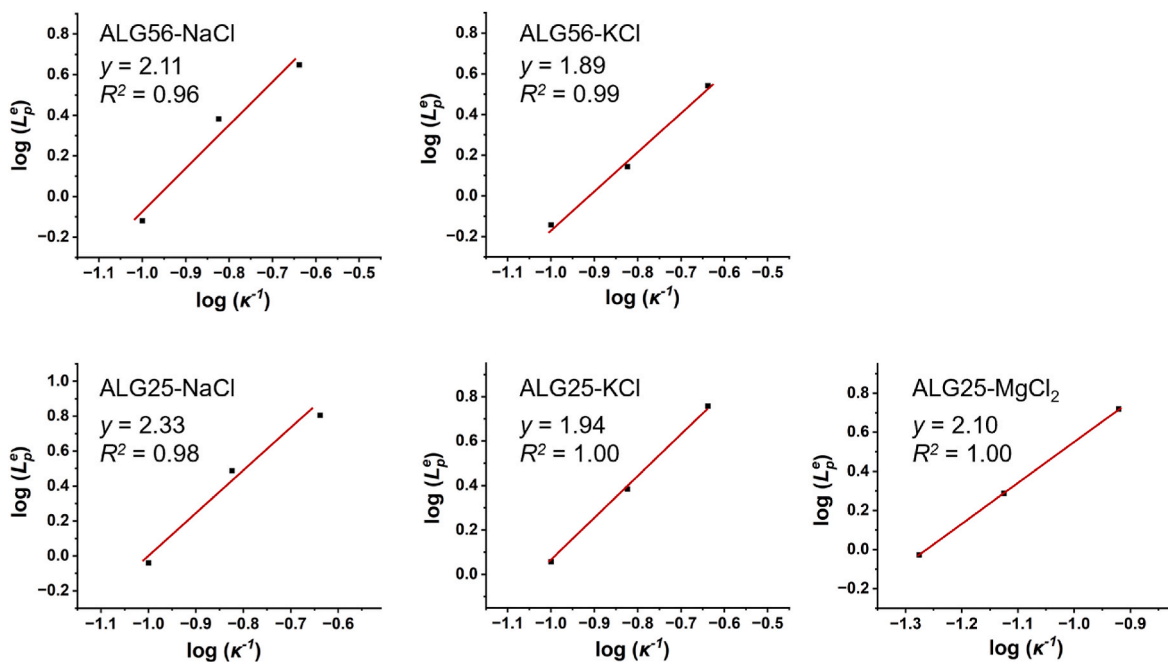


Fig. 6. Log-log plots of electrostatic persistence length ( $L_p^e$ ) as a function of the Debye screening length ( $\kappa^{-1}$ ) for ALG56 and ALG25 with different types of salts ( $\text{Na}^+$ ,  $\text{K}^+$  and  $\text{Mg}^{2+}$ ). Since the persistence length of ALG56 with 10 mM  $\text{Mg}^{2+}$  is taken as the  $L_p^0$ , the linear fit of the ALG56- $\text{Mg}^{2+}$  plot cannot be carried out.

In this case, the change in the chain structure can hardly be interpreted by the Debye-Hückel theory alone, which takes into account electrostatic interactions in a mean-field manner, thus avoiding an explicit treatment of counterions and salt ions (Odijk, 1977; Skolnick & Fixman, 1977). Instead, the overcharging and ion-ion correlations could explain the nonmonotonic behavior of persistence length.

Overcharging is a phenomenon where excessive counterions are adsorbed on the polyelectrolyte surface than required for neutralization. According to Manning condensation theory, for sodium alginate (monovalent charged groups and counterions), when the charge-density parameter  $\xi$  (also referred to as Manning parameter) before condensation is greater than unity, counterions are expected to condense on alginate chains until the  $\xi$  value is equal to unity (Manning, 1969; Wei & Hsiao, 2010). The charge-density parameter  $\xi$  is the number of unit charges per Bjerrum length along the chain contour (Limbach & Holm, 2001):

$$\xi = l_B/A$$

Where  $A$  is the distance between two charges along the chain contour. For sodium alginate,  $A = l_{unit} = M_{mono}/M_L = 198/424 \approx 0.5$  nm, where  $l_{unit}$  is the unit length,  $M_{mono}$  is the average monomer molecular weight (198 g mol<sup>-1</sup> for both mannuronate and guluronate),  $M_L$  is the mass per unit length (424 g mol<sup>-1</sup>•nm<sup>-1</sup> for alginate obtained from the chemical structure) (Vold et al., 2006; Cifre & de la Torre, 2014). The charge-density parameter of alginate can be calculated ( $\xi = 0.71/0.5 = 1.42$ ), which is greater than unity. Thus, counterion condensation occurred in salt-free alginate solutions and about 29.6% ( $1 - \xi^{-1}$ ) of monovalent counterions (sodium ions) were condensed on the alginate chain.

When the salt was added, the number of the condensed ions increased, leading to the collapse of the alginate chain. As the concentration of added salt exceeds the alginate-equivalent concentration, the alginate chain will be locally overcharged. The extra number of condensed ions results in the reexpansion of alginate chain rather than the collapse due to the ion excluded volume and the Coulomb repulsion between condensed ions (Limbach & Holm, 2001; Wei & Hsiao, 2007; Messina et al., 2002). With the addition of NaCl, KCl and MgCl<sub>2</sub>, the zeta potential values of alginate solutions all showed a decline trend but there was no charge inversion (Fig. S6). Although charge inversion could be used as the evidence of overcharging, many studies have reported that chain reexpansion could occur without charge inversion (Hsiao, 2006, 2008). It has been proved that charge inversion has no direct connection with the reexpansion of polyelectrolytes at high salt concentrations since overcharging does not necessarily result in charge inversion (Hsiao, 2006, 2008).

In addition, when salt concentration is greater than the alginate-equivalent concentration, there are non-condensed counterions in the bulk solution and thus ion-ion correlations become nonnegligible (Schefer et al., 2015). Free ions moving in the bulk solution can replace condensed ones on alginate chains dynamically, and alginate chains, which are collapsed due to the electrostatic screening effect, become expanded again to facilitate ion exchange. As the salt concentration increases, there will be more non-condensed counterions. Since the concentration gap between free and condensed ions increases, the frequency of ion exchange rises, and more alginate chains stay in an extended state, leading to an increase in the persistence length. Thus, both the overcharging and ion-ion correlations might play an important role in the increase of persistence length at high salt concentrations.

#### 4.3. Analysis of the change degree of persistence length

To analyze the difference of the flexibility of alginate chains affected by non-specific ions, the change degree  $\lambda$  of persistence length was calculated, which is the reduction rate of the persistence length at a certain salt concentration compared to that without salt added.

$$\lambda = (L_{p0} - L_p) / L_{p0} \times 100\%$$

where  $L_p$  and  $L_{p0}$  are the persistence length of alginate chains with salts at a certain concentration and at 0 mM, respectively. If the  $\lambda$  value is positive, the chain becomes more flexible; vice versa the chain gets stiffer. The greater the absolute value of  $\lambda$ , the larger the degree of variability in persistence lengths.

As shown in Fig. 7, the  $\lambda$  values of persistence length with different salt types and concentrations are all positive, indicating that compared with alginate chains in salt-free solution, the addition of salts results in a greater flexibility of chain. With the increase of salt concentration, the absolute values of  $\lambda$  go up and then down, suggesting a collapse-reexpansion transition. A positive  $\lambda$  value at high salt concentrations proves that the chain is not swollen back to its original size with no added salts. Furthermore, the relative magnitudes of the absolute values of  $\lambda$  for different salt types are in the order of  $\lambda(\text{Mg}^{2+}) > \lambda(\text{K}^+) > \lambda(\text{Na}^+)$  in the chain-collapse region, whereas in the chain-reexpansion region, the order follows:  $\lambda(\text{Na}^+) > \lambda(\text{K}^+) > \lambda(\text{Mg}^{2+})$ .

With the addition of salts, the electrostatic screening effect is enhanced, leading to a decrease in the intrachain electrostatic repulsion and a shortening of the persistence length, thus making the  $\lambda$  value positive. Since the electrostatic screening effect of divalent ion is stronger than that of monovalent ions (Conwell et al., 2003; Hsiao, 2006), Mg<sup>2+</sup> ions contribute more to the persistence length of alginate chains than K<sup>+</sup> and Na<sup>+</sup> ions, hence the absolute value of  $\lambda(\text{Mg}^{2+})$  is the largest. The effect of monovalent ions on alginate chains in solution is related to their binding ability which is dependent on the properties of ions itself (Zhang et al., 1998). Compared with Na<sup>+</sup> ions, K<sup>+</sup> ions possess a smaller hydration radius, indicating a stronger affinity for alginate chains, and therefore a more significant impact and a greater  $\lambda$  value. When excess salts are added, counterion condensation causes the reexpansion of the otherwise collapsed chains, leading to an increase in the persistence length and a decrease in the  $\lambda$  value. Overcharging has been reported to be enhanced with the increase in the radius of the ions (Ubbink & Khokhlov, 2004; Lyklema, 2006). Since Mg<sup>2+</sup> ions have the largest radius compared to K<sup>+</sup> and Na<sup>+</sup> ions, alginate chains in the presence of Mg<sup>2+</sup> ion are most reexpanded, resulting in the largest persistence length and the smallest  $\lambda$  value.

In addition, the absolute value of  $\lambda(\text{ALG56})$  is larger than that of  $\lambda(\text{ALG25})$  under the same salt environments, indicating that the persistence length of ALG56 decreases more than that of ALG25. Since ALG56 possesses a higher G content, it could be concluded that G unit

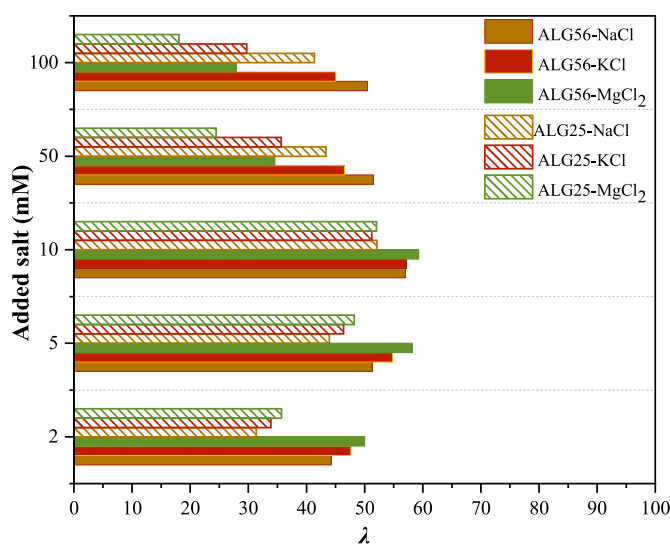


Fig. 7. The variation degree ( $\lambda$ ) of the persistence length ( $L_p$ ) of alginate chains with different salt types and concentrations.

has a stronger affinity for non-specific ions than M unit. Thus, by tuning the concentrations and types of salts, as well as the G content of alginate, the degree of chain collapse can be manipulated to achieve the desired functionality in practical applications.

## 5. Conclusions

In summary, this work provides direct experimental visualization for alginate chains on the molecular level in the presence of non-specific metal ions (NaCl, KCl and MgCl<sub>2</sub>) within a broad salt concentration range using high-resolution AFM. As hypothesized, with the salt concentration increasing, the morphology of ALG56 and ALG25 all shows a collapse-reexpansion transition, and the evolution of persistence length shows a nonmonotonic behavior. This differs from previous studies, which missed the reexpansion transition at high salt concentrations (Banerjee et al., 2022). Under low salt concentration condition, the collapse transition of alginate chains was induced by electrostatic screening effect. The electrostatic persistence length ( $L_p^e$ ) shows a strong dependence on the Debye screening length ( $\kappa^{-1}$ ) with a scaling relation of  $L_p^e \sim \kappa^{-2} \sim I^{-1}$ , which is consistent with the OSF theory. At high salt concentration, alginate chains reexpand, which could be explained by the overcharging and ion-ion correlations. Besides, the type of salt also affects the degree of change in persistence length, with magnesium ions (divalent ions) causing the greatest degree of collapse and reexpansion, followed by K<sup>+</sup> ions, and finally Na<sup>+</sup> ions. Since the degree of change in persistence length and height affected by salts was greater for ALG56 than for ALG25, it could be concluded that non-specific metal ions have a higher affinity for guluronate unit.

## CRedit authorship contribution statement

**Xiaoyang Li:** Writing – original draft, Methodology, Investigation, Formal analysis, Data curation. **Yi Wang:** Writing – original draft, Methodology, Investigation, Formal analysis, Data curation. **Cuixia Sun:** Writing – review & editing, Supervision, Data curation. **Yiguo Zhao:** Supervision, Formal analysis. **Wei Lu:** Supervision, Formal analysis. **Yapeng Fang:** Writing – review & editing, Supervision, Project administration, Funding acquisition, Conceptualization.

## Declaration of competing interest

The authors declare that they have no known competing financial interests or personal relationships that could have appeared to influence the work reported in this paper.

## Acknowledgments

This work was supported by National Natural Science Foundation of China (No. 32372269).

## Appendix B. Supplementary data

Supplementary data to this article can be found online at <https://doi.org/10.1016/j.foodhyd.2024.110744>.

## Data availability

Data will be made available on request.

## References

- Adamcik, J., Jung, J. M., Flakowski, J., De Los Rios, P., Dietler, G., & Mezzenga, R. (2010). Understanding amyloid aggregation by statistical analysis of atomic force microscopy images. *Nature Nanotechnology*, 5(6), 423–428.
- Banerjee, A., De, R., & Das, B. (2022). Hydrodynamic and conformational characterization of aqueous sodium alginate solutions with varying salinity. *Carbohydrate Polymers*, 277, Article 118855.
- Barrat, J. L., & Joanny, J. F. (1993). Persistence length of polyelectrolyte chains. *Europhysics Letters*, 24, 333–338.
- Barrat, J. L., & Joanny, J. F. (1996). Theory of polyelectrolyte solutions. *Advances in Chemical Physics*, 94, 1–66.
- Bennacef, C., Desobry-Banon, S., Probst, L., & Desobry, S. (2021). Advances on alginate use for spherification to encapsulate biomolecules. *Food Hydrocolloids*, 118, Article 106782.
- Caliskan, G., Hyeon, C., Perez-Salas, U., Briber, R. M., Woodson, S. A., & Thirumalai, D. (2005). Persistence length changes dramatically as RNA folds. *Physical Review Letters*, 95, Article 268303.
- Cao, L., Lu, W., Mata, A., Nishinari, K., & Fang, Y. (2020). Egg-box model-based gelation of alginate and pectin: A review. *Carbohydrate Polymers*, 242, Article 116389.
- Cifre, J. G. H., & de la Torre, J. G. (2014). Ionic strength effect in polyelectrolyte dilute solutions within the debye-hückel approximation: Monte Carlo and brownian dynamics simulations. *Polymer Bulletin*, 71, 2269–2285.
- Conwell, C. C., Vilfan, I. D., & Hud, N. V. (2003). Controlling the size of nanoscale toroidal DNA condensates with static curvature and ionic strength. *Proceedings of the National Academy of Sciences*, 100(16), 9296–9301.
- Dentini, M., Rinaldi, G., Risica, D., Barbetta, A., & Skjåk-Bræk, G. (2005). Comparative studies on solution characteristics of mannanuronic epimerized by C-5 epimerases. *Carbohydrate Polymers*, 59, 489–499.
- Dobrynin, A. V., & Rubinstein, M. (2005). Theory of polyelectrolytes in solutions and at surfaces. *Progress in Polymer Science*, 30, 1049–1118.
- Donati, I., & Christensen, B. E. (2023). Alginate-metal cation interactions: Macromolecular approach. *Carbohydrate Polymers*, 321, Article 121280.
- Fernando, I. P. S., Lee, W. W., Han, E. J., & Ahn, G. (2020). Alginate-based nanomaterials: Fabrication techniques, properties, and applications. *Chemical Engineering Journal*, 391, Article 123823.
- Hecht, H., & Srebnik, S. (2016). Structural characterization of sodium alginate and calcium alginate. *Biomacromolecules*, 17(6), 2160–2167.
- Hsiao, P. Y. (2006). Chain morphology, swelling exponent, persistence length, like-charge attraction, and charge distribution around a chain in polyelectrolyte solutions: Effects of salt concentration and ion size studied by molecular dynamics simulations. *Macromolecules*, 39, 7125–7137.
- Hsiao, P. Y. (2008). Overcharging, charge inversion, and reentrant condensation: Using highly charged polyelectrolytes in tetravalent salt solutions as an example of study. *The Journal of Physical Chemistry B*, 112, 7347–7350.
- Hu, C., Lu, W., Mata, A., Nishinari, K., & Fang, Y. (2021). Ions-induced gelation of alginate: Mechanisms and applications. *International Journal of Biological Macromolecules*, 177, 578–588.
- Liao, Q., Dobrynin, A. V., & Rubinstein, M. (2003). Molecular dynamics simulations of polyelectrolyte solutions: Nonuniform stretching of chains and scaling behavior. *Macromolecules*, 36, 3386–3398.
- Limbach, H. J., & Holm, C. (2001). End effects of strongly charged polyelectrolytes: A molecular dynamics study. *The Journal of Chemical Physics*, 114(21), 9674–9682.
- Lyklema, J. (2006). Overcharging, charge reversal: Chemistry or physics? *Colloids and Surfaces A: Physicochemical and Engineering Aspects*, 291, 3–12.
- Makarova, A. O., Derkach, S. R., Khair, T., Kazantseva, M. A., Zuev, Y. F., & Zueva, O. S. (2023). Ion-induced polysaccharide gelation: Peculiarities of alginate egg-box association with different divalent cations. *Polymers*, 15(5), 1243.
- Manning, G. S. (1969). Limiting laws and counterion condensation in polyelectrolyte solutions I. Colligative properties. *The Journal of Chemical Physics*, 51(3), 924–933.
- Messina, R., González-Tovar, E., Lozada-Cassou, M., & Holm, C. (2002). Overcharging: The crucial role of excluded volume. *Europhysics Letters*, 60(3), 383.
- Morch, Y. A., Donati, I., Strand, B. L., & Skjåk-Bræk, G. (2006). Effect of Ca<sup>2+</sup>, Ba<sup>2+</sup>, and Sr<sup>2+</sup> on alginate microbeads. *Biomacromolecules*, 7(5), 1471–1480.
- Odijk, T. (1977). Polyelectrolytes near the rod limit. *Journal of Polymer Science Polymer Physics Edition*, 15, 477–483.
- Odijk, T. (1979). Possible scaling relations for semidilute polyelectrolyte solutions. *Macromolecules*, 12(4), 688–693.
- Ramdhan, T., Ching, S. H., Prakash, S., & Bhandari, B. (2020). Physical and mechanical properties of alginate based composite gels. *Trends in Food Science & Technology*, 106, 150–159.
- Roiter, Y., Trotsenko, O., Tokarev, V., & Minko, S. (2010). Single molecule experiments visualizing adsorbed polyelectrolyte molecules in the full range of mono- and divalent counterion concentrations. *Journal of the American Chemical Society*, 132, 13660–13662.
- Santra, S., & Das, B. (2019). Counterion-binding and related phenomena in sodium alginate-sodium chloride-water ternary systems: A conductometric study. *Journal of Molecular Liquids*, 296, Article 111930.
- Schefer, L., Adamcik, J., & Mezzenga, R. (2014). Unravelling secondary structure changes on individual anionic polysaccharide chains by atomic force microscopy. *Angewandte Chemie International Edition*, 53(21), 5376–5379.
- Schefer, L., Usov, I., & Mezzenga, R. (2015). Anomalous stiffening and ion-induced coil–helix transition of carrageenans under monovalent salt conditions. *Biomacromolecules*, 16, 985–991.
- Sikorski, P., Mo, F., Skjåk-Bræk, G., & Stokke, B. T. (2007). Evidence for egg-box-compatible interactions in calcium – alginate gels from fiber X-ray diffraction. *Biomacromolecules*, 8(7), 2098–2103.
- Sim, A. Y. L., Lipfert, J., Herschlag, D., & Doniach, S. (2012). Salt dependence of the radius of gyration and flexibility of single-stranded DNA in solution probed by small-angle X-ray scattering. *Physical Review E*, 86, Article 021901.
- Skolnick, J., & Fixman, M. (1977). Electrostatic persistence length of a wormlike polyelectrolyte. *Macromolecules*, 10, 944–948.
- Smidsrød, O. (1970). Solution properties of alginate. *Carbohydrate Research*, 13(3), 359–372.

- Smidsrød, O., Glover, R. M., & Whittington, S. G. (1973). The relative extension of alginates having different chemical composition. *Carbohydrate Research*, *27*, 107–118.
- Smidsrød, O., & Haug, A. (1968). A light scattering study of alginate. *Acta Chemica Scandinavica*, *22*, 797–810.
- Smidsrød, O., & Haug, A. (1971). Estimation of the relative stiffness of the molecular chain in polyelectrolytes from measurements of viscosity at different ionic strengths. *Biopolymers*, *10*, 1213.
- Strand, K. A., Boe, A., Dalberg, P. S., Sikkeland, T., & Smidsrød, O. (1982). Dynamic and static light scattering on aqueous solutions of sodium alginate. *Macromolecules*, *15*, 570–579.
- Thu, B., Bruheim, P., Espevik, T., Smidsrød, O., SoonShiong, P., & SkjakBraek, G. (1996). Alginate polycation microcapsules: I. Interaction between alginate and polycation. *Biomaterials*, *17*(10), 1031–1040.
- Ubbink, J., & Khokhlov, A. R. (2004). Poisson-Boltzmann theory of the charge-induced adsorption of semi-flexible polyelectrolytes. *The Journal of Chemical Physics*, *120*, 5353–5365.
- Usov, I., Adamcik, J., & Mezzenga, R. (2013). Polymorphism complexity and handedness inversion in serum albumin amyloid fibrils. *ACS Nano*, *7*, 10465–10474.
- Usov, I., & Mezzenga, R. (2015). FiberApp: An open-source software for tracking and analyzing polymers, filaments, biomacromolecules, and fibrous objects. *Macromolecules*, *48*(5), 1269–1280.
- Varaprasad, K., Jayaramudu, T., Kanikireddy, V., Toro, C., & Sadiku, E. R. (2020). Alginate-based composite materials for wound dressing application: A mini review. *Carbohydrate Polymers*, *236*, Article 116025.
- Vold, I. M. N., Kristiansen, K. A., & Christensen, B. E. (2006). A study of the chain stiffness and extension of alginates, in vitro epimerized alginates, and periodate-oxidized alginates using size-exclusion chromatography combined with light scattering and viscosity detectors. *Biomacromolecules*, *7*, 2136–2146.
- Wang, Y., Zhao, Y., He, J., Sun, C., Lu, W., Zhang, Y., & Fang, Y. (2023). Doubling growth of egg-box structure during calcium-mediated molecular assembly of alginate. *Journal of Colloid and Interface Science*, *634*, 747–756.
- Wei, Y. F., & Hsiao, P. Y. (2007). Role of chain stiffness on the conformation of single polyelectrolytes in salt solutions. *The Journal of Chemical Physics*, *127*, Article 064901.
- Wei, Y. F., & Hsiao, P. Y. (2010). Effect of chain stiffness on ion distributions around a polyelectrolyte in multivalent salt solutions. *The Journal of Chemical Physics*, *132*, Article 02490.
- Zhang, H., Zheng, H., Zhang, Q., Wang, J., & Konno, M. (1998). The interaction of sodium alginate with univalent cations. *Biopolymers*, *46*(6), 395–402.